01 Jan 2007

Evaluation of Laser-Assisted Bremsstrahlung with Dirac-Volkov Propagators

Erik Lotstedt

Ulrich D. Jentschura
Missouri University of Science and Technology, ulj@mst.edu

Christoph H. Keitel

Recommended Citation

E. Lotstedt et al., "Evaluation of Laser-Assisted Bremsstrahlung with Dirac-Volkov Propagators," *Physical Review Letters*, vol. 98, no. 4, pp. 043002-1-043002-4, American Physical Society (APS), Jan 2007.
The definitive version is available at https://doi.org/10.1103/PhysRevLett.98.043002

Evaluation of Laser-Assisted Bremsstrahlung with Dirac-Volkov Propagators

Erik Lötstedt,* Ulrich D. Jentschura, and Christoph H. Keitel

Max-Planck-Institut für Kernphysik, Saupfercheckweg 1, D-69117 Heidelberg, Germany

(Received 27 July 2006; revised manuscript received 19 October 2006; published 22 January 2007; publisher error corrected 23 January 2007)

We study spontaneous bremsstrahlung emission in a highly intense laser field. In this regime the interaction with the laser field has to be treated nonperturbatively by using the relativistic formalism including Dirac-Volkov propagators, while the interaction with the Coulomb field and the bremsstrahlung radiation can be treated in first-order perturbation theory. For the intermediate electron state a fully laser-dressed propagator is used, including radiative corrections to avoid singularities on the mass shell. We find that the use of the Dirac-Volkov propagator is crucial to obtain correct numerical results. The cross section of the process is evaluated for laser intensities of order 10^{20} W/cm^2 and relativistic energies of the initial electron.

DOI: 10.1103/PhysRevLett.98.043002 PACS numbers: 32.80.Wr, 34.80.Qb

Theoretical investigations, together with numerical evaluation of basic quantum electrodynamic processes in the presence of a strong laser field, have recently gained in importance due to the availability of high-power lasers. Although analytical treatments of these processes started more than 40 years ago, accurate numerical evaluations are very demanding and have only recently become possible. Concrete numerical evaluations are, however, necessary to be able to make any precise comparisons or predictions, since the formulas resulting from the formalism are very complex. Calculations performed in this way are also important because they provide an alternative to numerically solving the Dirac equation, which requires considerable computer power [1,2]. The first process to be studied was laser-induced Compton scattering [3–5], followed by Mott scattering of a laser-dressed electron by the Coulomb field of a nucleus [6,7]. These first-order processes are relatively well studied, both analytically and numerically.

With increasing laser intensity, the contribution from second-order processes such as bremsstrahlung becomes more important. Reliable evaluations of second-order effects are important not only as fundamental processes but also for the understanding of dense laser-irradiated plasmas [8], and can also elucidate the process of high harmonic generation [9–11]. In the treatment of second-order processes with two vertices it becomes necessary to use intermediate, virtual states of the electron and of the photon. Because of the laser, it becomes in certain kinematic regimes possible that the intermediate particle goes on shell, i.e., satisfies the energy-momentum relation of a real particle, and creates a resonance peak in the cross section. These resonances will even be formally infinite, and to obtain finite results, additional, nonperturbative effects have to be included. The first second-order process to be studied analytically, and to some extent numerically, was electron-electron scattering [12–14]. Here the numerical treatment is less demanding since the intermediate state is the photon propagator, which can be well approximated by the free photon propagator. Also, resonant Compton scattering was investigated in [15], although no concrete numerical evaluations were performed. Finally, bremsstrahlung in a laser field was analytically studied in [16], where the process was formally treated. The laser-assisted bremsstrahlung process, in which a laser-dressed electron first emits a photon of arbitrary frequency and then interacts with a Coulomb potential, or the other way around, is described by the Feynman diagrams in Fig. 1. Here the intermediate electron can become real, which as we will see, due to the vanishing of the denominator in the electron propagator, results in a resonance peak in the cross section. The interpretation, due to Roshchupkin [16], is that when the intermediate electron goes on shell, the second-order bremsstrahlung process becomes the product of two first-order processes, namely, laser-induced Compton scattering and laser-assisted Coulomb scattering. As a result, the frequency of the emitted radiation obeys a modified Compton formula.

In this Letter, we consider a numerical evaluation of the laser-assisted bremsstrahlung process, which to our knowledge is the first concrete numerical evaluation ever of a second-order laser-dressed quantum electrodynamic process involving the Dirac-Volkov propagator. We present the fully relativistic formula for the matrix element, using the laser-dressed electron propagator. As usual, the laser-electron interaction is taken into account exactly by using Volkov states as the initial and final wave functions, whereas the interaction with the emitted radiation and

FIG. 1. Feynman diagrams describing laser-assisted bremsstrahlung. The laser-dressed electron and laser-dressed electron propagator are drawn as zigzag lines, the virtual Coulomb photon as a dashed line, and the bremsstrahlung photon as a wavy line.

with the Coulomb field is treated in first-order perturbation theory. As opposed to [16], where only approximate formulas for a weak laser field were obtained, we will evaluate the cross section for high laser intensities giving the electron a ponderomotive energy larger or even much larger than the rest mass of the electron. This work was also motivated by the question if the laser-dressed propagator can be approximated by the free electron propagator. We find that for high harmonics emission, this is not the case.

In the following, we use units where $\hbar = c = \epsilon_0 = 1$, the four-vector dot product is denoted by a dot: $x \cdot y = x_0 y_0 - \boldsymbol{x} \cdot \boldsymbol{y}$, and the "Feynman dagger" dot product with Dirac gamma matrices is written with a hat: $\hat{B} \equiv B \cdot \gamma$. The electron mass is denoted by m and the charge of the electron by $e = -|e|$. We consider a laser field with linear polarization, described by the vector potential $A^\mu = a\epsilon^\mu \cos\phi$, with $\mu \in \{0, 1, 2, 3\}$. Here $\phi = k \cdot x$, $k = (\omega, \boldsymbol{k})$ is the wave vector of the laser, and ϵ^μ is the polarization four-vector satisfying $\epsilon \cdot k = 0$ and $\epsilon^2 = -1$. As initial and final states, we employ the well-known Volkov wave functions $\psi_{i,f}(x)$ [17,18], which are solutions to the Dirac equation: $[i\hat{\partial} - e\hat{A}(\phi) - m]\psi_{i,f}(x) = 0$. These functions are characterized by the average momentum $q_{i,f} = p_{i,f} + e^2 a^2 k/(4k \cdot p_{i,f})$, with effective mass $m_*^2 = q_{i,f}^2$ and $p_{i,f}$ being the momentum of the electron outside the laser beam. The effective energy is denoted by $Q_{i,f} = q_{i,f}^0$. To be able to perform the required space-time integration, the Volkov wave functions have to be expanded into an infinite sum of plane waves with generalized Bessel functions as coefficients, which renders numerical treatment of processes involving Volkov states demanding. For the intermediate states we need the laser-dressed propagator of the electron [3,19]. The form suitable for our problem is presented in [20,21], where the propagator is written as $G(x, x') = (2\pi)^{-4} \times \int d^4p E(x, p) G_p^f \bar{E}(x', p)$. Here G_p^f is the free electron propagator in momentum space and $E(x, p)$ is a matrix similar to the Volkov wave function. For details, see Ref. [21].

Using the Volkov wave functions $\psi_{i,f}(x)$ and the laser-dressed Green's function together with the vector potential $A_C^\mu(x) = -Ze\delta^{\mu 0} e^{-|\boldsymbol{x}|/l}/(4\pi|\boldsymbol{x}|)$ of the screened Coulomb field with screening length l, the vector potential $A_b^\mu(x) = \varepsilon_{b,\lambda}^\mu e^{ik_b \cdot x}/(\sqrt{2\omega_b})$ describing the emitted bremsstrahlung photon with polarization $\lambda \in \{1, 2\}$ and wave vector $k_b = (\omega_b, \boldsymbol{k}_b)$, we can write down the transition matrix element S_{fi} in the first Born approximation, corresponding to the diagrams in Fig. 1:

$$
\begin{aligned}
S_{fi} &= -ie^2 \int d^4x_1 d^4x_2 \bar{\psi}_f(x_2)[\hat{A}_b(x_2) G(x_2, x_1) \hat{A}_C(x_1) + \hat{A}_C(x_2) G(x_2, x_1) \hat{A}_b(x_1)]\psi_i(x_1) \\
&= \sum_{n,s=-\infty}^{\infty} \frac{2\pi i Z e^3 m}{\sqrt{2\omega_b Q_i Q_f}} \frac{\delta(Q_f - Q_i + n\omega + \omega_b)}{\boldsymbol{q}_n^2 + l^{-2}} \bar{u}_f \Bigg[M_{fiff}^{-s}(\hat{\varepsilon}_{b,\lambda}) \frac{\hat{\tilde{p}}_f - \hat{k} e^2 a^2/(4k \cdot \tilde{p}_f) + m}{\tilde{p}_f^2 - m_*^2 - 2im\Gamma_{k \cdot q_f}[(\omega_b - s\omega)/Q_f] + 2im\Gamma_{k \cdot k_b}} \\
&\quad \times M_{ifif}^{-s-n}(\gamma^0) + M_{fiif}^{s+n}(\gamma^0) \frac{\hat{\tilde{p}}_i - \hat{k} e^2 a^2/(4k \cdot \tilde{p}_i) + m}{\tilde{p}_i^2 - m_*^2 - 2im\Gamma_{k \cdot q_i}[(s\omega - \omega_b)/Q_i] - 2im\Gamma_{k \cdot k_b}} M_{iiii}^{s}(\hat{\varepsilon}_{b,\lambda}) \Bigg] u_i,
\end{aligned} \tag{1}
$$

where

$$
\begin{aligned}
M_{jklm}^s(X) &= A_0^{sjk} X + A_1^{sjk} \left(X \frac{\hat{k} e a \hat{\epsilon}}{2k \cdot \tilde{p}_l} + \frac{e a \hat{\epsilon} \hat{k}}{2k \cdot p_m} X \right) \\
&\quad + A_2^{sjk} \frac{e a \hat{\epsilon} \hat{k}}{2k \cdot p_m} X \frac{\hat{k} e a \hat{\epsilon}}{2k \cdot \tilde{p}_l},
\end{aligned} \tag{2}
$$

with $A_N^{sjk} = A_N(s, \alpha_{p_j} - \alpha_{\tilde{p}_k}, \beta_{p_j} - \beta_{\tilde{p}_k})$, $j, k, l, m \in \{i, f\}$, $\alpha_p = ea\epsilon \cdot p/(k \cdot p)$, $\beta_p = -e^2 a^2/(8k \cdot p)$, $X \in \{\hat{\varepsilon}_{b,\lambda}, \gamma^0\}$. The generalized Bessel functions are defined through $A_0(s, \alpha, \beta) = \sum_n J_{2n+s}(\alpha) J_n(\beta)$, $A_N(s, \alpha, \beta) = (1/2)[A_{N-1}(s-1, \alpha, \beta) + A_{N-1}(s+1, \alpha, \beta)]$, where $J_n(\alpha)$ is the usual Bessel function. The momentum transfer from the Coulomb field is denoted by $\boldsymbol{q}_n = \boldsymbol{q}_f - \boldsymbol{q}_i + n\boldsymbol{k} + \boldsymbol{k}_b$, the two four-momenta of the virtual electrons by $\tilde{p}_f = q_f - sk + k_b$ and $\tilde{p}_i = q_i + sk - k_b$, and $u_{i,f}$ is a constant spinor. We have also included the small imaginary correction proportional to Γ_ρ, which results from the self-energy of a laser-dressed electron [12,15,16], and is related to the total probability of Compton scattering of an electron in a laser field. The inclusion of the nonperturbative term Γ_ρ in the denominators solves the problems of evaluating the differential cross section in kinematic regions where the electron goes on shell. According to our calculations, Γ_ρ is a linear function of the parameter ρ even for quite large values of a and is simple to include in numerical calculations. As will be discussed below, a large screening length l is introduced to cut off Coulomb singularities in a well-defined way. Energy conservation is expressed by the relation $Q_f = Q_i - n\omega - \omega_b$, meaning that the final electron with effective energy Q_f has exchanged n laser mode photons with the laser field. The summation over n is limited from above by the condition $Q_f \geq m_*$. Because of the neglection of the recoil of the nucleus, there is no momentum conservation. Note also that we choose to evaluate the process in the rest frame of the nucleus. That the matrix element is gauge invariant both under $\epsilon \rightarrow \epsilon + \Lambda_1 k$ and $\varepsilon_b \rightarrow \varepsilon_b + \Lambda_2 k_b$, where $\Lambda_{1,2}$ is an arbitrary constant, is most easily seen before carrying out the Bessel function expansion, by using the orthogonality and completeness relations of the Volkov wave functions [21]. We also see that when the condition $\tilde{p}_{f,i}^2 = m_*^2$ is satisfied, the intermediate electron becomes real, with a resonance peak in the cross section as a result. This con-

dition can be solved to obtain the frequencies where the resonances will occur:

$$\omega_b^f = \frac{sq_f \cdot k}{q_f \cdot n_b - sk \cdot n_b}, \qquad \omega_b^i = \frac{sq_i \cdot k}{q_i \cdot n_b + sk \cdot n_b}, \quad (3)$$

if $k_b^\mu = \omega_b n_b^\mu$. Here s appears as an index numbering the peaks. The peak at ω_b^i is precisely the frequency of the light emitted in the process of laser-induced Compton scattering [4,5], exhibiting the once controversial intensity-dependent frequency Doppler shift and photon recoil effect [5,22,23]. Because of the Doppler shift, the distance between the peaks will depend on the direction of $\boldsymbol{k}_b$, but also on the intensity of the laser field. In general, larger intensities will give smaller spacing between the peaks.

As mentioned above, generally momentum is not conserved. However, at bremsstrahlung frequencies ω_b^i satisfying Eq. (3) for some s, there will be a direction of the final electron so that momentum is conserved, that is, $\boldsymbol{q}_n = 0$ for $n = -s$. It follows that Eq. (3) is also satisfied for ω_b^f, with $s = -n$. When momentum is conserved, due to the slow falloff of the potential, the matrix element goes to infinity in the case of a naked Coulomb field. This means that if we integrate the differential cross section over the direction of the final electron, we will have singular peaks at frequencies satisfying Eq. (3). To regularize these singularities, we use a screened Coulomb potential. The screening length is chosen large enough to only affect the matrix element at the peaks, so that the difference between the screened and the bare Coulomb cross section at off-resonance values of ω_b is negligible.

We have evaluated the differential cross section resulting from the matrix element (1) for different directions of the final photon and different laser intensities. We sum over electron and photon polarizations, and we also integrate the differential cross section over the solid angle Ω_f of the outgoing average momentum $\boldsymbol{q}_f$. The resulting cross section will therefore be differential only in the bremsstrahlung frequency ω_b and in the bremsstrahlung solid angle Ω_b. The initial electron counterpropagates with the laser beam, i.e., $\boldsymbol{k}/\omega = -\boldsymbol{q}_i/|\boldsymbol{q}_i|$, and the angle between $\boldsymbol{q}_i$ and $\boldsymbol{k}_b$ is denoted by θ_b, with $\boldsymbol{k}_b$ lying in the plane spanned by $\boldsymbol{k}$ and $\boldsymbol{\epsilon}$. The spectrum for $\theta_b = 179°$ is shown in Fig. 2. Since this direction of the bremsstrahlung photon corresponds almost to the direction of the laser, harmonics of the laser frequency are expected. However, as can be seen from the graph, the magnitude of the peaks falls off quickly, and harmonics are only visible up to the 13th order. As expected, the cross section is composed of a number of high peaks, exceeding the field-free cross section [24,25] with several orders of magnitude, and a noncoherent background of comparable magnitude. At a certain order, the peaks can no longer overtake the background and disappear. For other directions of the final photon, the situation changes. Figures 3 and 4 show the spectra for $\theta_b = 1°$ and $\theta_b = 90°$. Here the peaks survive much longer, although they are no longer harmonics of the laser frequency in the lab frame. The spacing between the peaks is here larger than the laser frequency ω. It should be stressed that the mechanism responsible for the emission of harmonics here is not the well-known (re-)scattering of the electron by the nucleus, which is suppressed due to the acceleration of the electron in the laser propagation direction at our laser intensities, but rather laser-induced Compton scattering of the laser-dressed electron passing the nucleus without being deflected at all or with a very small deflection.

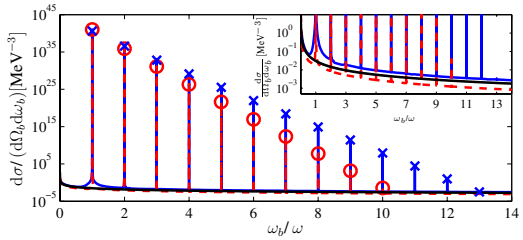

FIG. 2 (color online). The cross section for $\theta_b = 179°$, differential in bremsstrahlung frequency and solid angle. The laser frequency is $\omega = 1.17$ eV, the energy of the initial electron outside the laser is 10 m, $Z = 1$ and $l = 10^6 r_0$, where r_0 is the Bohr radius. This screening length corresponds to the separation of particles in ultrahigh vacuum, i.e., a pressure of 3×10^{-8} Pa at room temperature. The intensities used are $I = 5.2 \times 10^{20}$ W/cm^2 for the blue solid line, $I = 4.3 \times 10^{19}$ W/cm^2 for the red dashed line, and $I = 0$ for the black solid line. For clarity, the value of the cross section at the peaks is shown with a circle for the red dashed line, and with a cross for the blue solid line. The inset shows a magnification at small values of the cross section, to enable comparison between the background curves. At the intensities considered, the classical ponderomotive energy U_p is considerably larger than the rest mass of the electron. We have, for example, $U_p/m = 107.5$ for $I = 5.2 \times 10^{20}$ W/cm^2, which is clearly in the relativistic regime.

We also compared the cross section obtained by employing the free electron propagator in the matrix element with the fully laser-dressed cross section. Naïvely one would expect the replacement of the laser-dressed propagator

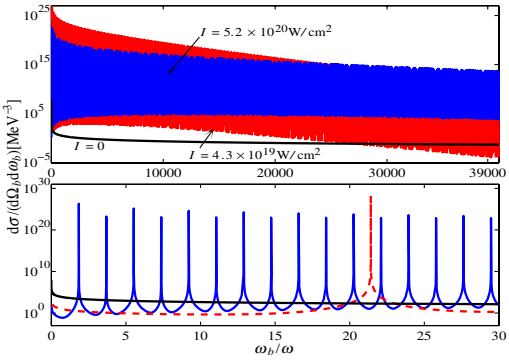

FIG. 3 (color online). The cross section for $\theta_b = 1°$, and otherwise the same parameters as in Fig. 2. In the lower close-up graph, the different line styles correspond to the same laser intensities as in Fig. 2. The positions of the peaks correspond to ω_b^i of Eq. (3) and the magnitude of the peaks is seen to decrease exponentially.

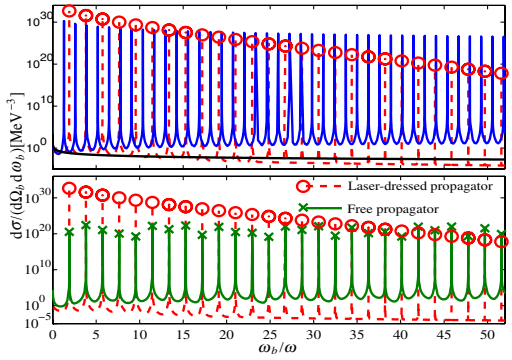

FIG. 4 (color online). The differential cross section for $\theta_b = 90°$, and otherwise the same parameters as in Fig. 2. In the upper graph, the different line styles correspond to the same laser intensities as in Fig. 2, and the peak values are shown with circles for the red dashed line. Here the intensity dependence on the peak spacing is not so strong compared to the case with $\theta_b = 1°$. In the lower graph comparing the laser-dressed and the free propagator, the intensity used is $I = 4.3 \times 10^{19}$ W/cm^2. For clarity, the peak values of the cross section are shown with crosses for the free propagator and with circles for the laser-dressed propagator.

with the free electron propagator $G_f(x, x') = (2\pi)^{-4} \times \int d^4p e^{-ip\cdot(x-x')}/(\hat{p} - m_* + i0)$, with the poles shifted to $p^2 = m_*^2$, to be a reasonable approximation, if the time between the interaction with the Coulomb potential and the bremsstrahlung radiation is short or if the frequency of the emitted photon is much higher than the laser frequency. Analytically one can show that for very high frequencies $\omega_b \gg Q_i$, the approximate and the fully laser-dressed cross section do indeed coincide, but at these frequencies the cross section is already in the cutoff region and therefore vanishingly small. The details about the cutoff, which decides the maximal bremsstrahlung energy, will be presented elsewhere. For moderate values of ω_b, as is shown in Fig. 4, where the condition $\omega_b \gg Q_i$ is not satisfied, there is no reason to assume good agreement. As discussed previously, for values of ω_b where the peaks are visible, the largest contribution to the matrix element occurs at vanishing Coulomb momentum $\boldsymbol{q}_n$. In absence of the Coulomb interaction, the emission part of the laser-dressed bremsstrahlung matrix element essentially reduces to the matrix element for laser-induced Compton scattering [4]. We recall that a Volkov state is a superposition of harmonic plane waves with quasi four momenta. A Volkov state can thus be regarded as an electron-laser bound system, with four-momentum levels labeled by an integer n, corresponding to the different plane-wave components. The amplitude of each level is roughly constant up to a certain $|n|$, above which the amplitude drops quickly. Compton scattering can be viewed as spontaneous photon emission and a transition between two levels of the electron-laser system. Momentum and energy conservation fix the four-momentum difference between these levels, and to obtain the total amplitude one has to sum coherently over all allowed transitions. For very small frequencies $\omega_b < \omega$, the amplitudes add up constructively, but for larger frequencies destructive interference between the different emission channels gives rise to the exponential decrease seen in Fig. 4, also expected classically [26]. However, when the free propagator is applied, the dominant transition is forced to occur between an initial level and a single, specific level with four-momentum close to the mass shell $p^2 = m_*^2$. The amplitude of this single "allowed" transition is approximately constant in the considered range of ω_b, as evident from Fig. 4. The completely different behavior of the fully laser-dressed process is thus explained by the additional emission channels.

E. L. is grateful to S. Schnez for helpful discussions. U. D. J. acknowledges DFG support (Heisenberg program).

*Electronic address: Erik.Loetstedt@mpi-hd.mpg.de

[1] A. Maquet and R. Grobe, J. Mod. Opt. **49**, 2001 (2002).
[2] Y. I. Salamin, S. X. Hu, K. Z. Hatsagortsyan, and C. H. Keitel, Phys. Rep. **427**, 41 (2006).
[3] L. S. Brown and T. W. B. Kibble, Phys. Rev. **133**, A705 (1964).
[4] A. I. Nikishov and V. I. Ritus, JETP **19**, 529 (1964).
[5] P. Panek, J. Z. Kamiński, and F. Ehlotzky, Phys. Rev. A **65**, 022712 (2002).
[6] M. M. Denisov and M. V. Fedorov, JETP **26**, 779 (1968).
[7] P. Panek, J. Z. Kamiński, and F. Ehlotzky, Phys. Rev. A **65**, 033408 (2002).
[8] C. Fortmann, R. Redmer, H. Reinholz, G. Röpke, A. Wierling, and W. Rozmus, High Energ. Dens. Phys. **2**, 57 (2006).
[9] M. Protopapas, D. G. Lappas, C. H. Keitel, and P. L. Knight, Phys. Rev. A **53**, R2933 (1996).
[10] D. B. Milosevic, S. Hu, and W. Becker, Phys. Rev. A **63**, 011403(R) (2000).
[11] J. Gao, F. Shen, and J. G. Eden, Phys. Rev. Lett. **81**, 1833 (1998).
[12] V. P. Oleĭnik, JETP **25**, 697 (1967).
[13] J. Bös, W. Brock, H. Mitter, and T. Schott, J. Phys. A **12**, 715 (1979).
[14] P. Panek, J. Z. Kamiński, and F. Ehlotzky, Phys. Rev. A **69**, 013404 (2004).
[15] V. P. Oleĭnik, JETP **26**, 1132 (1968).
[16] S. P. Roshchupkin, Sov. J. Nucl. Phys. **41**, 796 (1985).
[17] D. M. Volkov, Z. Phys. **94**, 250 (1935).
[18] V. B. Berestetskii, E. M. Lifshitz, and L. P. Pitaevskii, *Quantum Electrodynamics* (Pergamon, New York, 1982).
[19] H. R. Reiss and J. H. Eberly, Phys. Rev. **151**, 1058 (1966).
[20] V. I. Ritus, Ann. Phys. (N.Y.) **69**, 555 (1972).
[21] H. Mitter, Acta Phys. Austriaca Suppl. **14**, 397 (1975).
[22] T. W. B. Kibble, Phys. Rev. **138**, B740 (1965).
[23] J. H. Eberly and H. R. Reiss, Phys. Rev. **145**, 1035 (1966).
[24] H. A. Bethe and W. Heitler, Proc. R. Soc. A **146**, 83 (1934).
[25] R. L. Gluckstern and M. H. Hull, Jr., Phys. Rev. **90**, 1030 (1953).
[26] Y. I. Salamin and F. H. M. Faisal, Phys. Rev. A **54**, 4383 (1996).